AGU PUBLICATIONS

Water Resources Research

RESEARCH ARTICLE
10.1002/2017WR021626

BAM: Bayesian AMHG-Manning Inference of Discharge Using Remotely Sensed Stream Width, Slope, and Height

M. W. Hagemann[1], C. J. Gleason[1], and M. T. Durand[2]

[1]Department of Civil and Environmental Engineering, University of Massachusetts, Amherst, MA, USA, [2]School of Earth Sciences and Byrd Polar and Climate Research Center, Ohio State University, Columbus, OH, USA

Key Points:
- A new method is presented for estimating discharge using satellite observations
- The method uses Bayesian inference via hydraulics-derived likelihood and empirical priors from existing data sources
- Performance improvements over previous estimation algorithms are demonstrated on benchmark data sets

Supporting Information:
- Supporting Information S1
- Data Set S1

Correspondence to:
M. Hagemann,
mhageman@umass.edu

Citation:
Hagemann, M. W., Gleason, C. J., & Durand, M. T. (2017). BAM: Bayesian AMHG-Manning inference of discharge using remotely sensed stream width, slope, and height. *Water Resources Research*, *53*, 9692–9707. https://doi.org/10.1002/2017WR021626

Received 28 JUL 2017
Accepted 28 OCT 2017
Accepted article online 3 NOV 2017
Published online 24 NOV 2017

Abstract The forthcoming Surface Water and Ocean Topography (SWOT) NASA satellite mission will measure water surface width, height, and slope of major rivers worldwide. The resulting data could provide an unprecedented account of river discharge at continental scales, but reliable methods need to be identified prior to launch. Here we present a novel algorithm for discharge estimation from only remotely sensed stream width, slope, and height at multiple locations along a mass-conserved river segment. The algorithm, termed the Bayesian AMHG-Manning (BAM) algorithm, implements a Bayesian formulation of streamflow uncertainty using a combination of Manning's equation and at-many-stations hydraulic geometry (AMHG). Bayesian methods provide a statistically defensible approach to generating discharge estimates in a physically underconstrained system but rely on prior distributions that quantify the a priori uncertainty of unknown quantities including discharge and hydraulic equation parameters. These were obtained from literature-reported values and from a USGS data set of acoustic Doppler current profiler (ADCP) measurements at USGS stream gauges. A data set of simulated widths, slopes, and heights from 19 rivers was used to evaluate the algorithms using a set of performance metrics. Results across the 19 rivers indicate an improvement in performance of BAM over previously tested methods and highlight a path forward in solving discharge estimation using solely satellite remote sensing.

1. Introduction

Discharge through the world's rivers is one of the most fundamental quantities of relevance to hydrologic science, yet its accurate quantification remains elusive. Direct calculation of discharge requires simultaneous measurement of stream cross-sectional area and velocity. Such in situ measurement necessarily involves substantial human effort, restricting the spatial and temporal resolution of direct-measurement discharge data sets. Determining discharge at higher spatiotemporal resolution thus relies on estimation methods that calculate discharge as a function of more easily obtainable quantities. Continuous stream gauges achieve arbitrarily high temporal resolution by combining online sensors with empirical stage-discharge rating curves. These empirical relationships are based on interpolations and extrapolations of in situ measurements and provided such calibration data exist in sufficient quantities, commonly achieve accuracy within 5% of true discharge (Kennedy, 1984). Similar empirical relationships, approximated as simple power laws, form the basis of at-a-station hydraulic geometry (AHG), the equations of which relate stream height, width, and velocity to discharge via two site-specific, time-invariant parameters. Gleason and Smith (2014) discovered further relationships between the parameters of AHG across multiple cross sections within a stream in a set of equations termed at-many-stations hydraulic geometry (AMHG). Like AHG, AMHG describes a relationship between a single hydraulic variable (herein: width) and discharge but invokes fewer site-specific parameters and as a result has proved attractive in remote-sensing applications (Gleason et al., 2014).

Human effort is required to install, maintain, and routinely calibrate stream gauges and determine the parameters of A(M)HG, skewing the spatial distribution of discharge data sets toward more easily accessible waterways near civilization. The substantial costs involved further create disparities between countries and regions, with poorer countries often having few operational stream gauges. Moreover, the competition for scientific funding often results in existing gauges being taken off line, and the total number of active gauges worldwide has been in decline since the early 1970s (Hannah et al., 2011; Tourian et al., 2013). Geopolitics are an additional hindrance to progress, as discharge monitoring entities are often unwilling to make data available to people outside their own nation (e.g., Gleason & Hamdan, 2015).

Satellite remote sensing holds tremendous potential to overcome these barriers, providing measurements independent of human geography. Once in orbit, additional observations can be made and processed with minimal human effort. Optical sensors and synthetic aperture radar (SAR) provide satellite measurements of stream width and areal extent, while radar altimeters provide measurements of height and slope. Many studies have demonstrated reliable discharge estimation using empirical relationships between these satellite-measured variables and in situ measured discharge (Bjerklie et al., 2005; Brackenridge et al., 2005; Smith et al., 1996). However, these are only applicable where in situ data exist and therefore suffer the same drawbacks already described. Others have used satellite observations as input to established hydraulic equations (e.g., Manning's; Birkinshaw et al., 2014; Durand et al., 2010; Garambois & Monnier, 2015; LeFavour & Alsdorf, 2005), or assimilated them with numerical hydraulic models (Andreadis et al., 2007; Biancamaria et al., 2011; Durand et al., 2008; Neal et al., 2009; Yoon et al., 2012). Gleason et al. (2014) and Gleason and Smith (2014) demonstrated an AMHG-based discharge estimation method using satellite-observed widths only. Unfortunately, these methods all involve parameters that are unobtainable using existing remote-sensing methods and require some guesswork a priori.

The upcoming (2021) Surface Water and Ocean Topography (SWOT) satellite mission represents the state of the art in hydrologic monitoring from space. Each overpass of the satellite will measure stream width, height relative to ellipsoid, and slope for major rivers worldwide, setting the challenge of how best to model stream discharge using these quantities. Multiple approaches have already been proposed for turning SWOT measurements into streamflow estimates (e.g., Durand et al., 2014; Garambois & Monnier, 2015; Gleason et al., 2014). A common paradigm that has emerged relies on two tools: the inversion of flow-law equations (e.g., Manning's, Chezy), and the conservation of mass at the river-segment scale, wherein multiple cross sections (or reach-scale averages) can be defined and their geometry measured by SWOT. This paradigm, termed mass-conserved flow-law inversion (McFLI) has several variants, but all invoke at least one flow-law equation and mass conservation (Gleason et al., 2017). A recent paper (Durand et al., 2016) compared 5 McFLI algorithms using a data set of SWOT-observable variables from 19 major rivers distributed throughout the globe. The set of algorithms consisted of at-many-stations hydraulic geometry (AMHG; Gleason & Smith, 2014), GaMo (Garambois & Monnier, 2015), MetroMan (Durand et al., 2014), and two novel methods termed mean flow and geomorphology (MFG) and mean flow and constant roughness (MFCR). While at least one algorithm achieved the targeted performance criterion of 35% relative root-mean-square error (RRMSE) on 14 of the 19 rivers in the data set, the median RRMSE was 55%, and no single algorithm achieved the targeted performance on more than six rivers, revealing the scale of the challenge in obtaining accurate estimates of discharge using only SWOT-available data.

The present study was undertaken to improve on the state of McFLI in two main ways. First, rather than using a single flow law, we combine a physical/empirical flow-law (Manning's equation) with a geometric/empirical flow law (AMHG) in a synergistic framework. We term this the Bayesian AMHG-Manning, or BAM, approach. Each of these flow laws has been previously and independently used to estimate discharge with varying degrees of efficacy, and all of the algorithms in Durand et al. (2016) used one or the other as the basis of McFLI. Second, in order to overcome the issue of an underconstrained system of equations, we place the BAM in a fully Bayesian mathematical setting, beginning with empirically derived descriptions of uncertainty. This is a departure from previous AMHG-based discharge algorithms (e.g., Gleason et al., 2014) and allows for the quantification of uncertainty in estimates of discharge and other parameters. More importantly, this approach also allows for prior information to be taken from external data sets—even those that do not include SWOT-observable measurements. The Bayesian discharge estimation algorithm we describe is flexible (as it is able to be parameterized from multiple sources), computationally efficient, and explicit in its treatment of uncertainty.

2. Data and Methods

2.1. Data

The 19 test cases described in Durand et al. (2016) were used for model development and validation in this study. Like the eventual SWOT satellite data product, each test case included both a cross-section product and a reach-averaged product, containing stream width, height, and surface slope for multiple locations (cross sections or reaches) and days. As described in Durand et al. (2016), these "data sets" are

derived from hydraulic modeling and therefore constitute simulated values forced by measured flows, stream bathymetry, and downstream water elevations. Gauge-measured daily discharge was also provided for validation purposes. These 19 data sets represent rivers that span a range of hydraulic and hydrologic regimes, and previous results indicate that the combined test data represent a challenge for discharge estimation. The number of reaches per simulation ranged from 3 to 16, the number of cross sections ranged from 7 to 3188, and the number of days ranged from 24 to 367. For the sake of clarity, references to these synthetic "observations" or "measurements" will be placed in quotations, as in this sentence.

Bayesian methods require certain constraints in their unknown parameters; these are imposed as "prior" probability distributions. BAM derived its prior distributions on flow-equation parameters (including discharge) from acoustic Doppler current profiler (ADCP) measurements at 10,081 USGS gauging stations (Canova et al., 2016). Exact distributions obtained from this data set are described in section 2.3. This so-called "hydroSWOT" database was produced by USGS for the purpose of assessing information about flow-equation quantities not directly observable by the SWOT satellite but useful for determining relationships between SWOT-observable and other hydrologic variables such as cross-sectional area and discharge.

Finally, a data set containing width and discharge measurements from a physiographically diverse set of 34 rivers was used to compare the BAM to previously obtained AMHG-based discharge estimation results (Gleason et al., 2014). The flow component of this data set was obtained from in situ measurements, while the width component was derived from satellite imagery. These results represent the first and largest test of McFLI methods to date. Note that since slope and height are not included in these data, only the AMHG portion of BAM was operable (see section 2.2.1), offering a demonstration of BAM's flexibility and providing context to the value of additional measurements.

2.2. Bayesian Methods and Hydraulics

This section describes an algorithm for estimating discharge using the variables stream height, slope, and width—the quantities that will be measured by the SWOT satellite. For simplicity, we present the algorithm at the cross-section scale, but its application at the reach scale is identical. Bayesian probabilistic methods describe the probability distribution of an unknown quantity, conditional on the values of known quantities on which the desired unknown depends. Arrival at a solution via Bayesian inference is different from deterministic approaches in that what is obtained is not a single solution, but a description of the uncertainty structure, including which values are more and which are less likely to be the truth based on measurements and prior knowledge. While a single deterministic answer may be more desirable, it may also be impossible to obtain, for example when the mathematical system is underconstrained, as in McFLI. Discharge estimation in ungauged basins has long been framed in terms of "constraining uncertainty" (Sivapalan et al., 2003), and Bayesian methods provide a well-established formalization of this idea.

2.2.1. Hydraulic Equations

Two underlying flow equations were considered—Manning's equation and AMHG. These, together with conservation of mass, constitute the McFLI framework for discharge estimation.

At the multireach scale, if flow is assumed to be conserved and Manning's n assumed constant, we may write Manning's equation for daily-resolution discharge as

$$Q_t = \frac{1}{n} A_{it}^{5/3} W_{it}^{-2/3} S_{it}^{1/2} \tag{1}$$

where Q is discharge ($m^3\ s^{-1}$), A is cross-sectional area (m^2), W is width (m), S is slope (unitless), the index i specifies the cross section, and t specifies the day. A_{it} may further be split into a time-invariant unknown part, A_0 and a time-variant but measurable part, $\delta A_{it} = \sum_{t':W_{t'} \le W_t} W_{t'} \Delta H_{t'}$. Equation (1), along with the continuity equation, $Q_i = Q \forall i$, leads to a system of $N_x N_t$ equations with $N_x N_t + 1$ unknowns, where N_x is the number of distinct cross sections and N_t is the number of days observed.

AMHG describes a relationship between parameters of width-discharge rating curves at multiple cross sections within a single river segment (Gleason & Smith, 2014). The AMHG flow equation for discharge (Gleason & Wang, 2015) can be written

$$Q_t = \left(\frac{W_{it}}{W_c}\right)^{\frac{1}{b_i}} Q_c \tag{2}$$

where W_c and Q_c are AMHG global parameters and b_i is the at-a-station hydraulic geometry (AHG) width-discharge exponent for cross section i. (In AMHG, the AHG coefficient, a, drops out, and is equivalent to $W_c Q_c^{-b}$.) Invoking the conservation of mass yields a system of $N_x N_t$ equations with $N_x N_t + 2$ unknowns.

2.2.1.1. Bayesian Flow-Law Inversion

Bayesian inference methods obtain a probability distribution for unknown values (*parameters*) given a set of measured observations and known relationships between measured and unknown values. Formally,

$$p(\Theta|x) = \frac{f(x|\Theta)\pi(\Theta)}{\int f(x|\theta)\pi(\theta)d\theta} \tag{3}$$

where Θ is a particular set of parameters (including all N_t flows), $\pi()$ is the joint prior density for this parameter set, x is the observed data (including all $N_x N_t$ widths and other SWOT observations, depending on the flow law invoked), and $f()$ is the likelihood function of the observations given the parameters. In the denominator the integral is over all possible sets of parameters.

As the denominator is typically computationally prohibitive to integrate exactly, Bayesian inference methods require only that the equation is specified to a proportionality, i.e., $p(\Theta|x) \propto f(x|\Theta)\pi(\Theta)$, where $f(x|\Theta)$ is the *likelihood* of the data given the parameters Θ and $\pi(\Theta)$ is the *prior* distribution of the parameters Θ. Given this proportionality, the full posterior distribution can be approximated via Monte Carlo sampling.

In order to conceive of McFLI as a likelihood, we first note that even where all non-Q parameters of a flow law are known exactly, the discharge the equation obtains is still only an estimate of true discharge. Here we denote the flow-law-estimated discharge $\dot{Q}$, and the actual discharge Q. Further, we denote the flow-law error as $\epsilon = \log Q - \log \dot{Q}$. Assuming the flow-law equation to be an unbiased estimate of discharge, ϵ has a mean of zero and a standard deviation that is dependent on the flow law used and how well it represents the hydraulics of the river to which it is applied. In the BAM formulation, Q is a parameter; $\dot{Q}$ is not. Therefore, it is convenient to write:

$$\log \dot{Q} = \log Q - \epsilon \tag{4}$$

2.2.1.2. Manning's Equation

Manning's equation (equation (1)), when log-transformed and scaled to have integer coefficients, becomes

$$6 \log \dot{Q}_t = -6 \log n + 10 \log\left(\delta A_{it} + A_{0,i}\right) - 4 \log W_{it} + 3 \log S_{it} \tag{5}$$

In order to become a likelihood equation, we rearrange equation (5) to isolate the measured variables and substitute for the actual flow via equation (4):

$$4 \log W_{it} - 3 \log S_{it} = -6 \log n - 6 \log Q_t + 10 \log\left(\delta A_{it} + A_{0,i}\right) + 6\epsilon_m \tag{6}$$

where the additional subscript m specifies that this is error from Manning's equation. Since the right-hand side is a linear transformation of ϵ_m, a normal random variable, it is itself a normal random variable with mean $-6 \log n - 6 \log Q + 10 \log(\delta A + A_0)$ and standard deviation of $6\sigma_m$, where σ_m is the standard deviation of ϵ_m. The observations given on the left-hand side of equation (6) can be thought of as realizations of the random variable described on the right-hand side.

2.2.1.3. AMHG

When AMHG is log-transformed and rewritten as a likelihood, equation (2) becomes

$$\log W_{it} = b_i(\log Q_t - \log Q_c) + \log W_c + \epsilon_g \tag{7}$$

where $\epsilon_g$is the AMHG error. In this case the only measured variable is width, hence the single quantity on the left-hand side. This again yields a normal likelihood distribution with mean zero and standard deviation equal to σ_g. Since AMHG is a relatively newly described phenomenon, information about the distribution of ϵ_g is lacking. We approximated AMHG based on AHG error, which hydroSWOT estimated to have standard deviation equal to 0.22.

2.3. Prior Distributions on Unknown Parameters

Prior distributions specify the a priori uncertainty about an unknown parameter. We arrive at these distributions in four ways: by considering theoretical limits on their values, by observing statistics of these

quantities reported in published literature, by observing statistics obtained via the hydroSWOT database, and (in the case of Q_t) from a global water-balance model.

The number of required prior distributions depends on the flow law(s) used in the inversion. Both flow laws include $Q_t, t=1,\ldots,N_t$ as an unknown parameter. Manning's equation includes the additional unknown parameters $A_{0,i}, i=1,\ldots,N_x$ and n. For AMHG the parameters are W_c, Q_c, and $b_i, i=1,\ldots,N_x$. The combined Manning/AMHG method includes all of the parameters from both stand-alone versions.

2.3.1. Prior on Q_t

As described in Gleason et al. (2014), strict limits were imposed on Q_t based on an assumed minimum and maximum depth and velocity of each river, approximated as having a rectangular channel. Q_t was constrained to be between $W_{\min}d_{\min}v_{\min}$ and $W_{\max}d_{\max}v_{\max}$, where $W_{\min}$ and $W_{\max}$ are the observed minimum and maximum width, respectively, at each cross section, and $v_{\min}=0.5\mathrm{m/s}, v_{\max}=5\mathrm{m/s}, d_{\min}=0.5$ m, and $d_{\max}=10$ m. Within these constraints, which are appropriate for the large rivers in our data sets given the overestimation of flow area by our rectangular assumption, Q_t followed a truncated normal distribution centered at Q_{WBM}, the output of a global water-balance model (Wisser et al., 2010), and with a coefficient of variation of 1.

2.3.2. Prior on $A_{0,i}$

The hydroSWOT database contains measurements of flow, area, width, and stage for 10,081 stream cross sections throughout the United States, with a median of eight observations per cross section. A_0 in hydroSWOT was calculated as the minimum observed area for each cross section. Relationships between statistics of SWOT-observable variables and A_0 were quantified using multiple regression (Figure 1), yielding the following relationship between width statistics and A_0:

$$\log A_{0,i}=0.855+1.393\times\mathrm{mean}(\log W_{it})-1.7249043\times\mathrm{SD}(\log W_{it})+\epsilon_{A_0} \quad (8)$$

where the width statistics are calculated over the time index, and ϵ_{A_0} is an error term with standard deviation of 0.948. This relationship was found to have an R^2 of 0.70 (Figure 1a). As the errors of the above model were approximately normally distributed in the hydroSWOT database, this constrains the prior distribution on log A_0 to be normal with a mean given by the right-hand side and a standard deviation equal to the residual standard error.

2.3.3. Prior on Manning's n

Published values of Manning's n in natural rivers were used to constrain the prior distribution on n, which was taken to be lognormal with parameters $\mu=-3.5$ and $\sigma^2=1$. This results in a slightly right-skewed bell curve with 5th and 95th percentiles at $n=0.006$ and $n=0.156$, respectively, and with a median of 0.030.

2.3.4. Priors on W_c and Q_c

Little is yet known about physical meaning of the Q_c AMHG parameter. Yet if AMHG holds, this should be within the range of historic flow (Gleason & Wang, 2015). Thus, Q_c was given the same prior distribution as that of Q_t, described above. Where AMHG holds, W_c is strongly associated with the global average flow

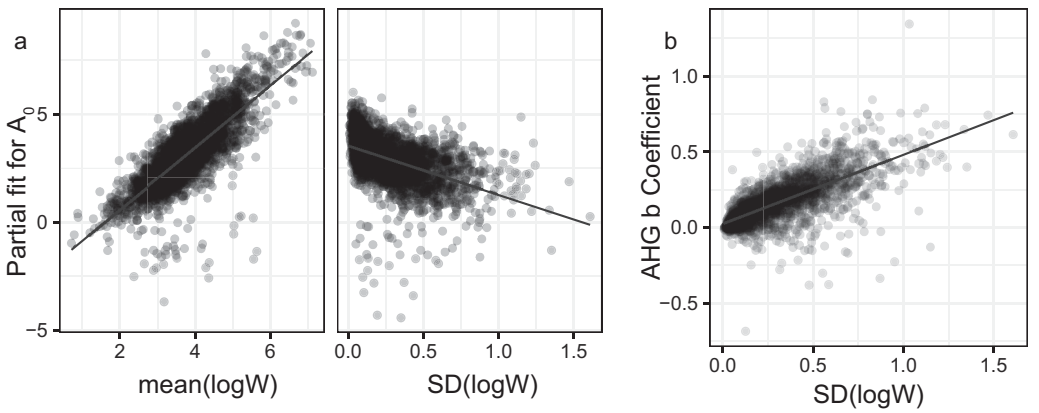

Figure 1. Regression plots for hydroSWOT-derived prior distributions as a function SWOT-observable quantities. (a) A_0 and (b) AHG b coefficient as a linear function of standard deviation of log-transformed width (a measure of a river's width variability), as used to obtain prior distribution ofr b_i in BAM. R^2 of regression is 0.55. Resulting prior distribution: normal with mean $\mu_b=0.02+0.458\mathrm{SD}(\log W)$, standard deviation $\sigma_b=0.098$.

(over space and time) for a given river segment. Thus, W_c was given a lognormal prior distribution centered on the mean observed W for the river segment and with a coefficient of variation of 0.01. Gleason and Wang (2015) suggested that Q_c and W_c are given as spatial modes of time-mean quantities at a station by mathematical definition, which Shen et al (2016) later showed to be sufficient but not necessary. Therefore, our choices for priors are consistent with this definition until more is revealed about AMHG.

2.3.5. Prior on b_i

The hydroSWOT database included observations necessary to calculate AHG width-discharge parameters, including b, for every station represented. This resulted in the following empirical relationship for AHG b, calculated across all hydroSWOT stations (Figure 1b):

$$\log\ b = 0.02161 + 0.4578SD(\log\ W) + \epsilon_b \tag{9}$$

Here again, ϵ_b is random error, this time with a standard deviation of 0.098. This gives b a normal prior distribution conditional on the standard deviation of observed (log-transformed) widths for a given cross section.

2.4. Bayesian AMHG and Manning (BAM) Algorithm

The prior and likelihood distributions described above are sufficient to state the Bayesian probability model for the unknown parameters conditional on the remotely sensed observations. Bayesian inference via Monte Carlo then involves drawing a sample from the specified distribution and calculating statistics (e.g., the mean) of this sample. Numerous algorithms exist to do the sampling, including Metropolis and Metropolis-Hastings (Durand et al., 2014; Gelman et al., 2014). A major drawback for these methods is the computational time required, which increases as the number of parameters grows larger. This study used an optimized Hamiltonian Monte Carlo method via the Stan Bayesian modeling language (http://mc-stan.org/). While this still involves sampling from a high-dimensional distribution, the steps taken within this multidimensional space are optimally and dynamically sized as to minimize the required computational effort (Betancourt & Girolami, 2015).

Four versions of the Bayesian AMHG and Manning (BAM) method were implemented on the 19-river SWOT simulation data: Manning-only, AMHG-only, Manning-with-AMHG, and Manning with an AMHG switch, triggered when a river exhibits behavior indicative of strong AMHG—namely width variability and a high p_{int}, the percentage of intersecting AHG curves (Gleason & Wang, 2015). This "Switch" algorithm operates as Manning-with-AMHG when both $\mathrm{SD}(\log\ W) > 0.1$ and $p_{int} > 0.15$, and Manning-only otherwise. The thresholds of 0.1 and 0.15 were used to comply with values in Durand et al. (2016) and Gleason and Wang (2015), respectively.

The AMHG-only BAM was additionally deployed on the 34-river width-discharge data set. Due to the lack of other SWOT-measureable variables in this data set (i.e., S, δA), the Manning-based BAM algorithms could not be applied to this data set.

2.5. Performance Metrics

Four performance metrics were used to assess performance of the BAM methods (Table 1). Two of these, relative RMSE (RRMSE) and relative bias (rBIAS), are equivalent to metrics used in Durand et al. (2016) and characterize, respectively, the spread and the central tendency of relative discharge errors. A third, "normalized" RMSE (NRMSE) was implemented to compensate for the fact that RRMSE is highly sensitive to

Table 1
Performance Metrics Used for Algorithm Evaluation

Description	Abbreviation	Definition
Relative root-mean-square error	RRMSE	$\sqrt{\frac{1}{N_t}\sum_{i=1}^{N_t}\left(\frac{Q_i-\hat{Q}_i}{Q_i}\right)^2}$
Normalized root-mean-square error	NRMSE	$\sqrt{\frac{1}{N_t}\sum_{i=1}^{N_t}\left(\frac{Q_i-\hat{Q}_i}{Q}\right)^2}$
Relative bias	rBIAS	$\frac{1}{N_t}\sum_{i=1}^{N_t}\left(\frac{\hat{Q}_i-Q_i}{Q}\right)$
Nash-Sutcliffe efficiency	NSE	$1-\sum_{i=1}^{N_t}\left(Q_i-\hat{Q}_i\right)^2/\sum_{i=1}^{N_t}\left(Q_i-\bar{Q}\right)^2$

baseflow errors that are small relative to peak flow, yet substantially inflate RRMSE. NRMSE differs from RRMSE in that it scales the RMSE by the mean flow, rather than scaling each individual residual by the true (measured) flow value. Finally, Nash-Sutcliffe efficiency (NSE) was added as a commonly used measure of model performance, reflecting the percent of variance in the original data set that is explained by the model.

3. Results

3.1. Synthetic Data Sets From Durand et al. (2016)

BAM was applied to both cross-section and reach-scale data sets produced by the simulations described in section 2.1. For conciseness, the focus herein will be on results at the reach scale (section 3.1.1), as this is most consistent with the methods applied in Durand et al. (2016). A summary comparison of BAM applied at the cross-section scale to the Durand et al. (2016) test cases is presented in section 3.1.2.

3.1.1. Reach-Scale Results

Hydrographs of BAM-estimated discharge (Figure 2) demonstrate overall close reproduction of synthetic "observed" flows, although the predictions on several rivers (e.g., Tanana, Upstream Garonne) were

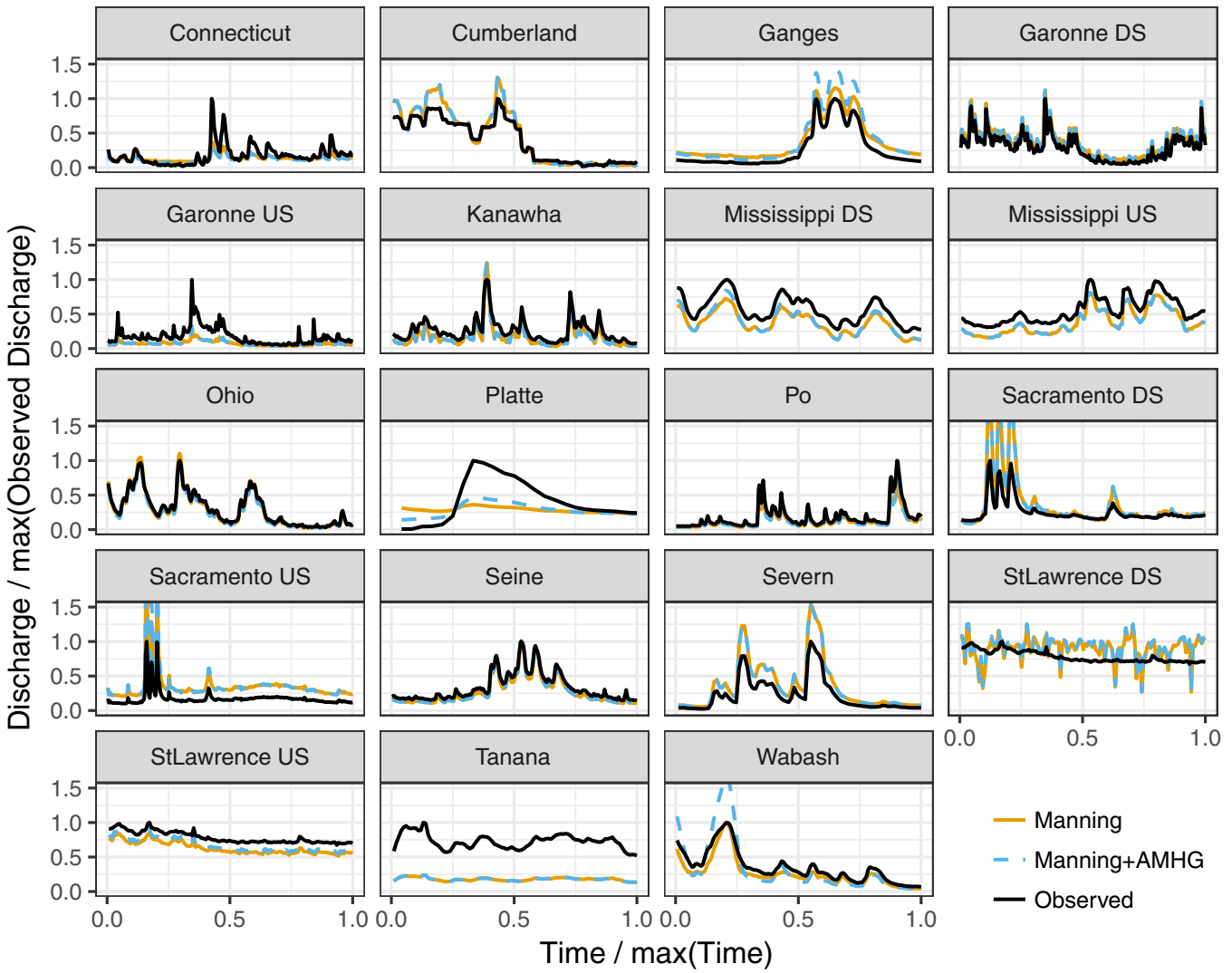

Figure 2. Synthetic "observed" and BAM-predicted (Manning-only and Manning-with-AMHG) streamflow for all rivers in validation data set, using reach-averaged data. US: upstream; DS: downstream.

noticeably biased. Manning-only and Manning-with-AMHG algorithms produced very similar results, although in several cases the Manning-with-AMHG predicted larger peak flows than Manning-only. In some cases (Mississippi Downstream, Platte) this made Manning-with-AMHG closer to synthetic "observed" flows, while in others (Wabash, Ganges) Manning-only was closer as a result. AMHG-only BAM hydrographs (not shown in Figure 2) were less accurate reproductions in many rivers, misrepresenting both the average flow and its variability.

Viewed in aggregate, the BAM-derived estimates of discharge correlated strongly with "measured" values, both in the Manning-only and Manning-with-AMHG versions (Figure 3). While individual rivers exhibit bias, the algorithm on the whole was unbiased across the entire set of 19 rivers. AMHG-only estimates were less strongly correlated with "observed" flows for most rivers. Moreover, many rivers display upward concavity in AMHG-only, overpredicting lowest and highest flows and underpredicting midrange flows. This indicates overestimation of AHG *b* for in-channel flows and underestimation of *b* for high, overbank flows. Nonetheless, BAM-AMHG tended to linearly approximate these nonlinear relationships reasonably well, suggesting that much if not most of the shortcomings of BAM-AMHG are the result of violations of A(M)HG assumptions, rather than a failure to reliably estimate its parameters.

The three different Manning-inclusive BAM variants (i.e., all BAMs except AMHG-only) performed similarly well across all performance statistics considered (Figure 4 and Table 2). Median performance statistic values for the Manning-only method were better than other BAMs across all statistics except rBIAS. None of the Manning-inclusive BAMs showed substantial bias, and median rBIAS values were within 19% of zero. The other statistics—NRMSE, RRMSE, and NSE—had skewed distributions with median values indicating good performance, but with severe underperformance for some rivers. Median NRMSE across rivers varied between 39% and 50%, but individual rivers' NRMSE ranged from 9% (for Connecticut) to 135% (for Upstream Sacramento). RRMSE ranged from 14% to 1,149%, with the median for each method ranging

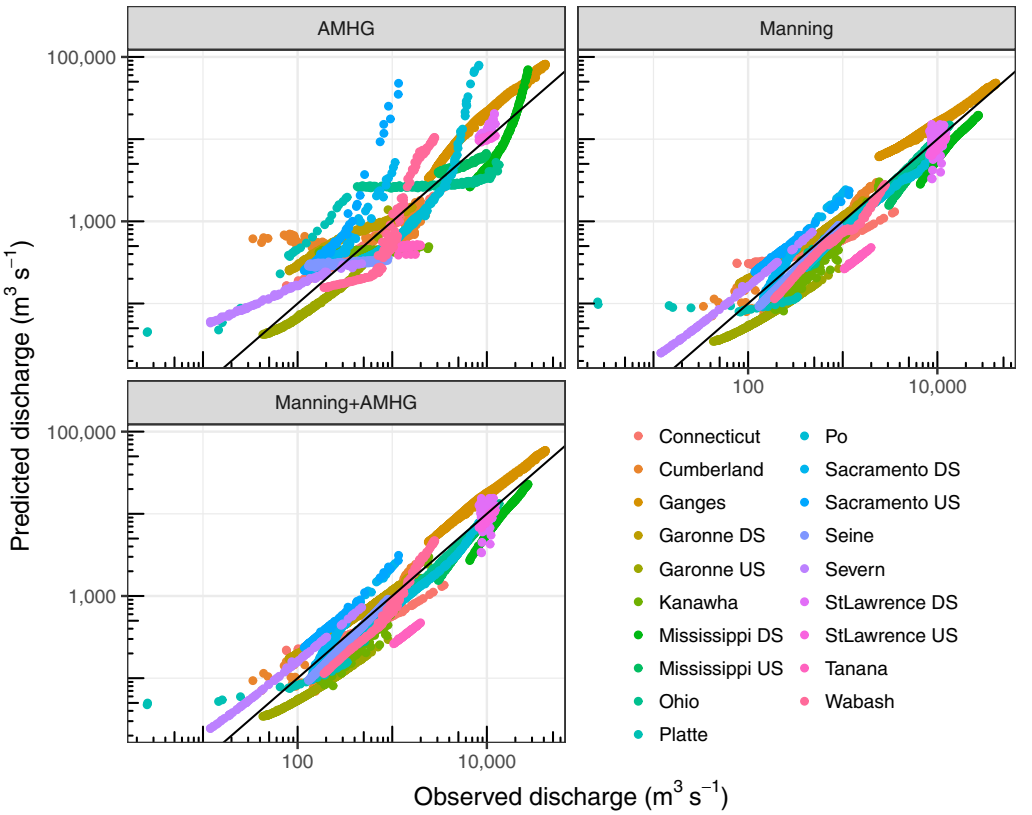

Figure 3. Scatterplots (log-log) of predicted versus synthetic "observed" discharge for two BAM variants, using reach-averaged data. The solid line indicates perfect prediction (prediction = observed). Points above the line indicate overprediction; points below the line indicate underprediction.

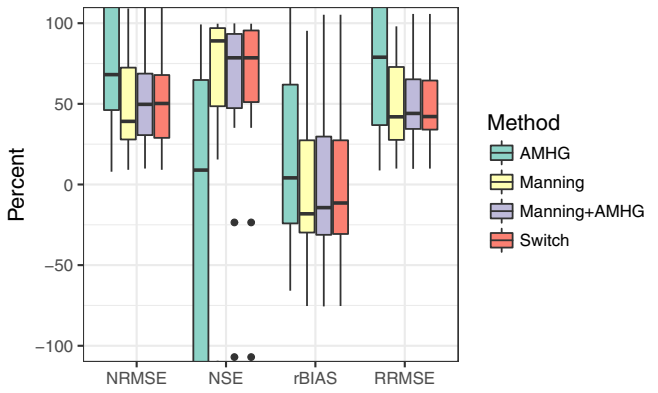

Figure 4. Boxplots of predictive performance statistics for BAM variants, using reach-averaged data. Statistics are as defined in Table 1. The Switch method is identical Manning + AMHG if SD of log(width) > 0.1 and p_{int} > 15%, and identical to Manning otherwise. The vertical axis is truncated and excludes statistics with values beyond ±100% (see Table 2).

between 42% and 44%. Median NSE was between 79% and 89%, yet all three methods had negative NSE values for some rivers.

Compared with previously reported statistics on the test data set from other estimation methods (Durand et al., 2016), the BAM methods outperformed nearly all on aggregate (again, with the exception of AMHG-only). BAM had more consistently good performance across all rivers if not reproducing some of the most accurate results of the Durand et al. (2016) intercomparison. Although Manning-inclusive BAMs' median bias across all rivers was worse than several previously reported methods, these BAMs had a tighter range than all previously reported methods except MFG, which was negatively biased on average (Figure 5a). All three Manning-inclusive BAMs also had lower median RRMSE than any previously reported method, and overall were distributed closer to zero, despite several previous methods having lower minimum RRMSE (Figure 5b).

The AMHG-only BAM had less consistently good performance across all performance statistics (Figures 5 and 6), reflecting the inaccuracies described above. While its median bias was the best across all BAM methods, AMHG-only had significant positive relative bias for many rivers, in excess of 200% in some cases (Table 2). Its RRMSE was comparable to the previous genetic algorithm implementation (Gleason & Smith, 2014), having similar median and minimum values.

3.1.2. Cross-Section-Scale Results

Use of finer-scale cross-section data yielded similar results to reach-averaged data when assessed by RRMSE and rBIAS (Figure 5). Cross-section BAM predictions had smaller median rBIAS, but a wider spread across the test cases. RRMSE was also similar, with predictions using cross-section data having slightly lower minimum values, in all cases except AMHG-only, and higher median values for both Manning-with-AMHG and Switch.

Table 2
Goodness of Fit Statistics for BAM Algorithms

	%NRMSE				%NSE				%rBias				%RRMSE			
River	A	A + M	M	S	A	A + M	M	S	A	A + M	M	S	A	A + M	M	S
Connecticut	23	61	62	62	92	51	57	57	−5	−24	−31	−31	27	69	48	48
Cumberland	62	30	31	30	43	88	87	88	−20	14	14	14	302	39	40	39
Ganges	142	46	73	73	0	99	83	83	94	45	58	58	86	95	77	77
Garonne DS	55	27	29	27	92	100	99	100	52	27	29	27	106	49	50	49
Garonne US	50	75	72	72	76	50	53	53	−36	−56	−54	−54	35	51	50	50
Kanawha	72	38	39	38	4	92	92	92	−31	−33	−34	−33	53	42	43	42
Mississippi DS	63	35	31	31	−224	96	99	99	−8	−34	−31	−31	52	37	36	36
Mississippi US	26	30	30	30	58	100	100	100	−13	−30	−30	−30	20	34	34	34
Ohio	76	9	16	9	20	99	99	99	−30	−4	−14	−4	152	14	21	14
Platte	553	75	60	60	−2,309	15	54	54	417	−31	−32	−32	596	1,113	522	522
Po	507	39	40	40	−2,898	90	92	92	56	−26	−30	−30	109	26	30	30
Sacramento DS	240	106	109	106	−1,019	−117	−132	−117	102	45	46	45	89	42	43	42
Sacramento US	1,902	109	135	135	−91,609	26	−107	−107	357	95	101	101	385	97	98	98
Seine	56	17	16	17	14	100	100	100	1	−17	−15	−17	61	22	21	22
Severn	61	83	80	80	81	72	74	74	39	60	59	59	183	74	72	72
StLawrence DS	30	28	30	28	−9	−422	−401	−422	27	14	18	14	28	30	31	30
StLawrence US	8	19	15	19	59	97	96	97	5	−19	−14	−19	9	20	15	20
Tanana	67	76	76	76	5	40	39	40	−66	−75	−76	−75	65	75	76	75
Wabash	224	27	53	53	−987	95	35	35	64	−23	−4	−4	103	27	38	38

Note. Statistics are as defined in Table 1. BAM variants abbreviated as follows: A, AMHG-only; A + M, AMHG + Manning; M, Manning-only; S, "Switch" (Switch chooses when it is appropriate to include AMHG in inversion, and is equivalent to A + M if river has SD(log W) > 0.1 and p_{int} > 15%, otherwise it is equivalent to M).

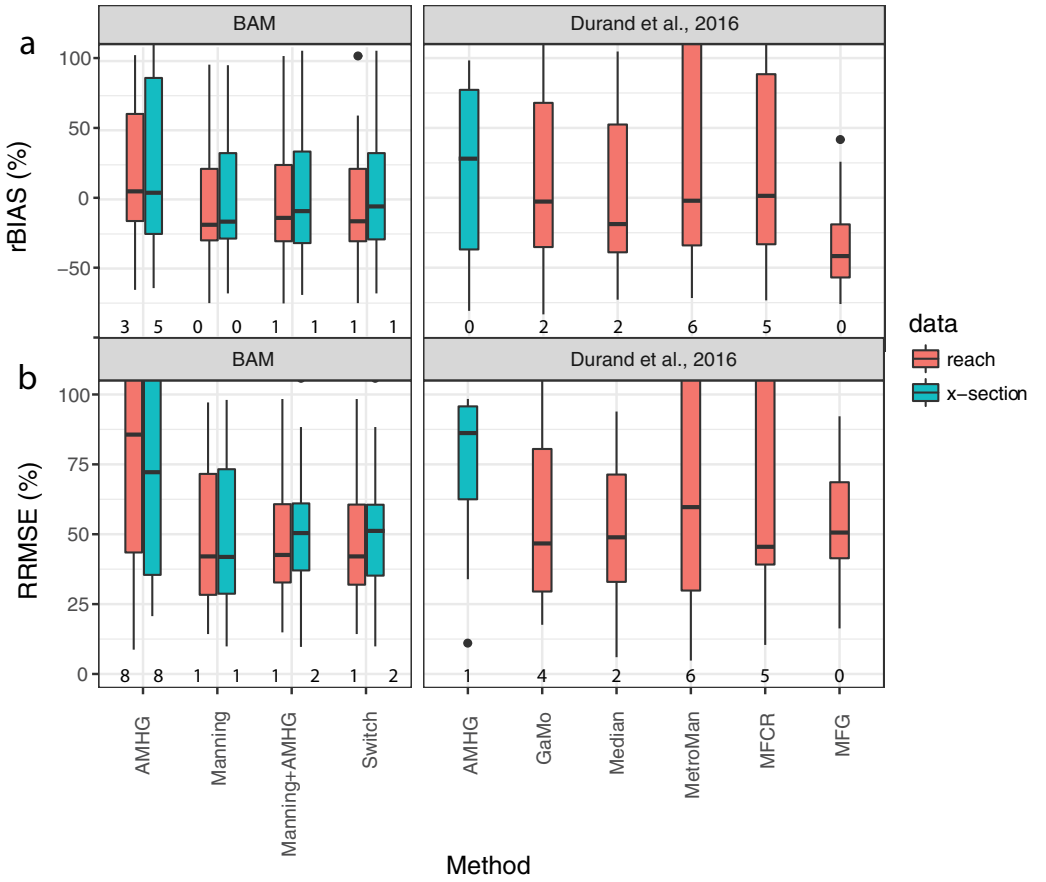

Figure 5. Performance metrics (as defined in Table 1) of various discharge algorithms, including BAM variants and those reported in Durand et al. (2016). (a) rBIAS: vertical axis is truncated to ±100%; numbers indicate the number of outliers above the plot area. (b) Percent RRMSE: vertical axis is truncated to 100%; numbers indicate the number of outliers above the plot area.

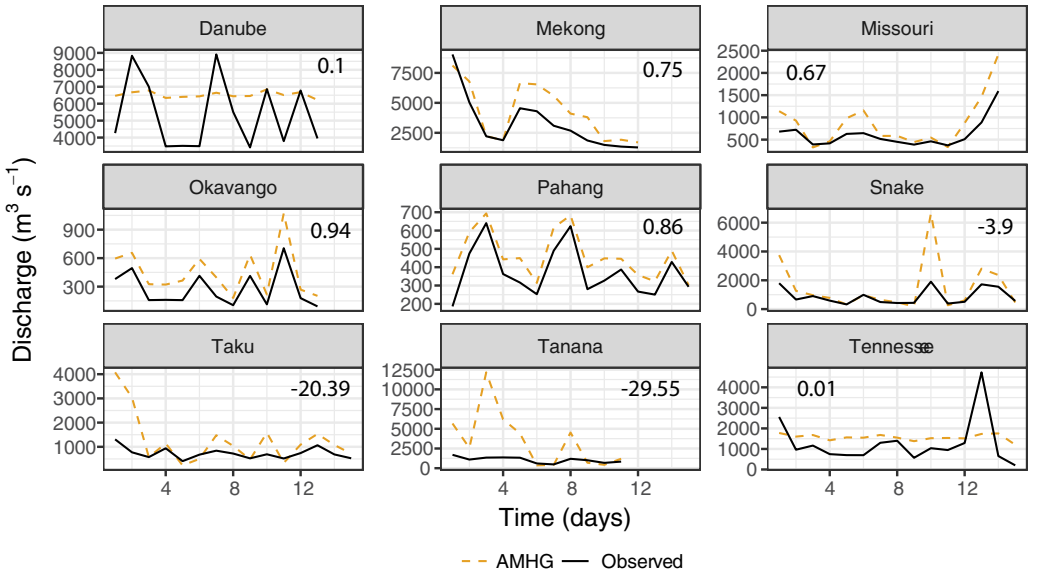

Figure 6. In situ measured and BAM-AMHG-predicted hydrographs for selected rivers in width-discharge only data set. Inset numbers are Nash-Sutcliffe efficiency (as a fraction). AMHG Q_c parameter was obtained using a prior distribution centered on water-balance model mean discharge (remote-sensed proxy Q_c results not shown on account of severe difference in scale).

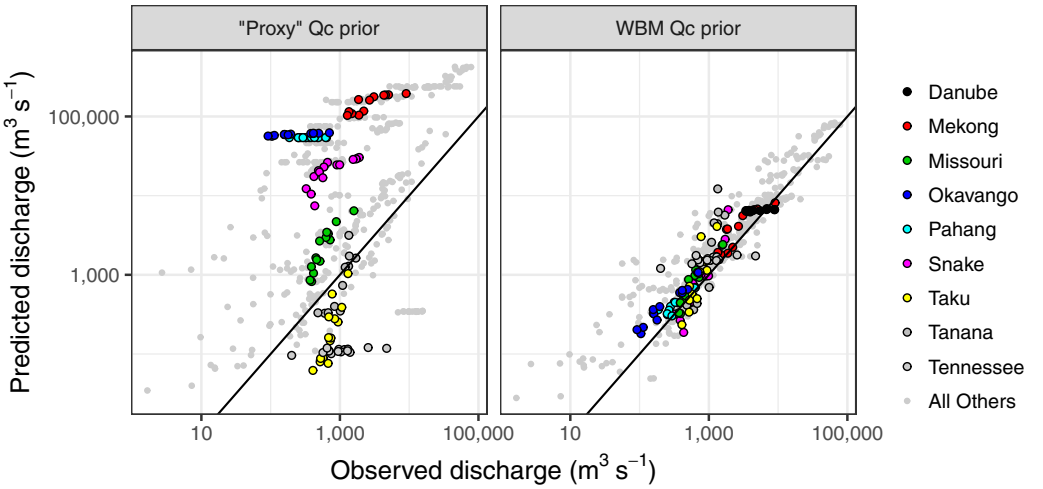

Figure 7. Scatterplots (log-log) of predicted versus observed discharge for AMHG-only on width-discharge data set, using different priors on Q_c prameter. Selected rivers from Figure 6 highlighted in color. (left) Q_c parameter obtained using the proxy described in Gleason and Smith (2014). (right) Q_c parameter obtained using a lognormal prior distribution centered on water-balance model output and with a coefficient of variation equal to 1.

3.2. Width-Discharge Data Set From Gleason et al. (2014)

Hydrographs of the AMHG-only BAM applied to the width-discharge data set (Figure 6) reveal mixed performance, with AMHG predictions being variously biased high (e.g., Missouri), biased low (e.g., Tennessee), more variable (Taku), or less variable (Danube) compared to observed hydrographs. As in the application to Durand et al. (2016) data sets, AMHG-only predictions on the width-discharge data set were somewhat biased high, tending more often to overpredict actual discharge (Figure 7).

Compared against a previous implementation of AMHG, which used a genetic algorithm to obtain discharge estimates on the same width-only data set, BAM-AMHG achieved on-average worse, but comparable performance. All of the BAM-AMHG RRMSE values lay within the range of the genetic algorithm RRMSE, and the BAM-AMHG maximum RRMSE (895%) was substantially lower than that for the genetic algorithm (6,416%), although the median RRMSE was lower for the genetic algorithm (Figure 8). In addition to the different inference method (genetic algorithm versus Bayesian), BAM-AMHG-only differed from previous AMHG implementations in its treatment of the Q_c parameter. Whereas BAM uses a prior distribution based on water-balance model average discharge, the genetic algorithm used a statistical proxy—now defunct—based on remote-sensed observations (Gleason et al., 2014). While this proxy proved a fortuitous choice for the genetic algorithm, replacing the BAM-AMHG prior with this proxy for Q_c did not improve its performance. On the contrary, using the proxy $Q_c$instead of the water-balance model Q_c prior severely biased the BAM-AMHG results, often by several orders of magnitude (Figure 7).

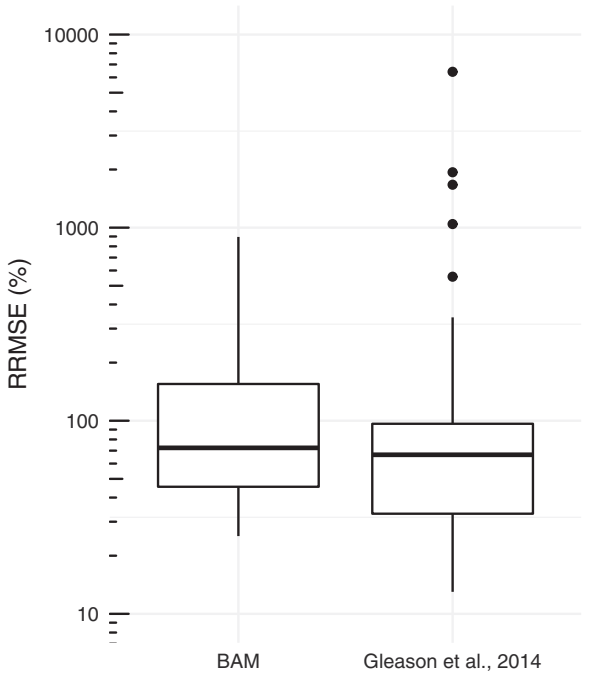

Figure 8. Boxplots of predictive performance, assessed by RRMSE, comparing BAM-AMHG-only implementation against genetic algorithm implementation from Gleason et al. (2014), using the width-only data set.

4. Discussion

4.1. The Case for Bayesian McFLI

The results of this study give continued reason to be optimistic about the use of Bayesian inference in obtaining accurate discharge estimates from SWOT-observable variables. The accuracy of BAM improves on existing benchmarks using other McFLI algorithms—with BAM achieving consistently low bias and RRMSE, despite BAM invoking no new hydraulics. The primary advantage of BAM arises from its

treatment of the uncertainty inherent in a physically unconstrained system. Rather than seeking an optimum heuristically, BAM invokes prior information from external data sets and prior published literature. Statistics from the hydroSWOT database constrained the prior distributions on A_0 and AMHG b, providing new information not available in previous McFLI implementations. In future refinements of BAM other parameters (e.g., Manning's n, AMHG Q_c) may be similarly constrained given the right data sets.

As reach-averaged quantities by definition contain less granular information than the cross-section-scale quantities from which they are derived, it may reasonably be expected that the enhanced resolution of cross-section data would lead to more accurate results. The SWOT mission will create reach averages largely to remedy substantial instrument noise at the cross-section scale, and it had previously been hypothesized that lackluster reach-scale McFLI results arose in part from this averaging (Durand et al., 2016). That the present study's results showed similar—and in some cases worse—performance using cross-section data may be viewed as a validation of reach-averaging as a noise-reducing feature.

As a Bayesian method, BAM relies on two components: likelihood functions, which describe the probability distribution from which observations are generated; and prior distributions representing a priori knowledge of unmeasured quantities such as discharge and base cross-sectional area. The likelihood functions underlying BAM arise directly from—and can be thought of as probabilistic representations of—McFLI. Flow-law inversion produces a set of $N_x N_t$ determinisitic equations of the form given in equations (1) and (2). Mass conservation, combined with assumptions on Manning error, reduces the number of unknown discharge parameters by a factor of N_x, and provides a simple likelihood function for SWOT-observable quantities, conditional on the unknown parameters. The SWOT observations are then realizations of the random process described by the McFLI likelihood functions.

There is good reason for McFLI to be conceived of probabilistically. Unless new as-yet undiscovered hydraulic equations are invoked that result in a fully constrained system, the number of potential solutions to McFLI equations using SWOT observations will be infinite. Yet it is unreasonable to treat every set of allowable parameters equally, for precisely the rationale that underlies Bayesian statistics: prior information constrains unknown quantities. BAM provides such a probabilistic formulation that is both mathematically concise and computationally feasible to arrive at a (probabilistic) solution. Once in this form, the resulting uncertainty of the solutions can be constrained via prior distributions obtained from external data sets and prior published literature.

The same insight—using external information to improve discharge estimates—has been considered in previous McFLI applications, albeit in a less explicit fashion. Gleason et al. (2014) considered AMHG dependence on hydrologic regime, differentiating arid-climate rivers and braided rivers as poor candidates for AMHG. The present study made no such differentiation, except in the Switch method, which differentiated width-variable from width-invariable rivers. Garambois and Monnier (2015) demonstrated greatly improved performance of their GaMo algorithm if even a single depth measurement is available. While it is unlikely such information will avail itself to SWOT, estimates of depth may be available using insights from hydroSWOT or other large-scale databases. Such estimates, even if not highly certain, can be incorporated into BAM by way of prior distributions.

The hydroSWOT database proved a highly useful tool in characterizing the prior distributions of certain BAM parameters. Despite the richness of this data set, neither Manning's equation, which relies on slope measurements, nor AMHG, which relies on multiple locations' width measurements within a river, could be fully characterized from hydroSWOT alone. Further refinement of BAM may be directed at assembling data sets from which Manning's n, W_c, Q_c, σ_m, and σ_g may be described probabilistically as a function of SWOT-observable quantities, as hydroSWOT provided for A_0 and b. Readily available technologies facilitate near-continuous slope measurement, either via submerged pressure transducers, or remote-sensing tools such as LiDAR and RADAR. AMHG parameters remain somewhat mysterious and are an active area of research, both empirical and theoretical. Both fronts will need to be advanced to make AMHG a mature predictive tool. On the empirical front, existing databases of gauge data may be mined for hydrologically connected series of width-discharge data sets, from which AHG and ultimately AMHG may be characterized. Ultimately, the use of databases such as hydroSWOT may miss important hydrologic regimes not captured by the sample of rivers they comprise. While hydroSWOT's data spans the entire United States and therefore contains information from a diverse array of physiographic environs, it is nonetheless geographically biased. Its

sample of high-order rivers, which are arguably the most important from a water-resources perspective, is especially small. More geographically diverse data sets should therefore be assembled and utilized in order to ensure BAM's parameters are adequately characterized for global water-resources assessment.

A previous Bayesian McFLI algorithm, MetroMan, used a Metropolis sampler and Mannings equation, and achieved very good performance on certain rivers in the Durand et al. (2016) data set. BAM constitutes a wholly different and more probabilistically motivated approach to Bayesian discharge estimation. While their differences are too many to enumerate here, some are worth noting. Fundamentally, MetroMan is conceived as an optimization algorithm, seeking to minimize the error in mass conservation. This optimization becomes a quasi-likelihood function, assumed to be Gaussian. As described in section 2.2.1, BAM assumes mass conservation outright, and instead obtains its likelihood functions from errors in the flow-law estimates of discharge. In other words, BAM includes uncertainty in the flow law, and is thus the difference between BAM and MetroMan equivalent to difference between strong and weak constraint in data assimilation (Talagrand, 2003). While this version of BAM did not consider measurement error, this would be straightforward to implement in future versions, and would result in a slight modification of the likelihood distribution. For example, if errors on log W and log S are assumed to be independent and their measurement errors have standard deviation σ_W and σ_S, respectively, then the Manning's likelihood distribution (equation (6)) would be modified to have a standard deviation equal to $\sqrt{\left(6\sigma_m\right)^2+\left(4\sigma_W\right)^2+\left(3\sigma_S\right)^2}$.

The conception of BAM from flow-law errors and empirically derived prior distributions results in several desirable properties in comparison to MetroMan. The mathematics are simpler, owing largely to log transformation prior to inference but also to the method's explicitly Bayesian formulation. As both the priors and likelihood for BAM are empirically derived and therefore verifiable probability distributions, the resulting posterior distribution is a more accurate representation of the uncertainty space. Finally, the BAM framework is flexible and expandable, allowing for potentially any flow law or combination of flow laws to be used synergistically.

The implementation of BAM using Hamiltonian Bayesian inference has no bearing on the results it obtains; a different implementation using the Metropolis algorithm would in theory yield the same posterior distribution of discharge and other parameters. However, by optimizing the sampling procedure, Hamiltonian Bayes converges more quickly and is less computationally intensive than other inference methods. While this makes BAM more attractive for application to SWOT data, it may not be computationally feasible in all situations. The computing time required is directly proportional to the number of parameters being estimated, and hence to the number of cross sections and days considered. While too few cross sections may yield less accurate results, too many will result in prohibitive computational time. This study circumvented this concern by using a random sampling of cross sections when N_x exceeded 30; more sophisticated selection of cross sections may improve performance, for example by providing a hydraulically diverse set of cross-sectional geometries.

4.2. BAM Performance

It is interesting to interpret Manning versus Manning + AMHG across performance metrics. Figure 4 shows that Manning alone had substantially lower median NRMSE and higher median NSE but comparable median RRMSE, suggesting it is a better option for discharge estimation. However, the Manning + AMHG is arguably more stable, given its smaller interquartile ranges in Figure 4 across metrics, and lower median bias. Here the Switch method is interesting, as it tends to successfully discriminate when AMHG should be added to the Manning inversion, choosing the variant with better RRMSE in 12 of 19 cases. By this criterion, Switch performance improves when the p_{int} threshold is raised to 0.2, selecting the better variant in 14 of 19 cases. Thus based on this study, it is recommended that in future studies the Switch method be applied with the above threshold; however, these values should be further investigated using a larger set of test cases.

It is known that AMHG does not hold in many rivers (Gleason & Wang, 2015), and attempting to apply it in such cases could result in Manning-derived flows becoming unnecessarily skewed. Even restricting the addition of AMHG to more width-variable rivers yielded underwhelming results, perhaps due to a flawed assumption that width variability is a reliable indicator of strong AMHG. Out-of-bank flow conditions could also affect performance; these conditions were included in the data despite being incongruent with AMHG's geometric underpinnings. Therefore, an update to the AMHG method would include an ability to discriminate when there is a switch in channel geometry and estimate b separately on either side of this switch.

This would necessitate a change in likelihood functions and increase the complexity of the problem, which might arguably move solutions farther away from reality. However, given large-scale flood modelling work, we might reasonably be able to constrain the out-of-bank flows with an appropriately defined accurate b prior. We leave this investigation for a future study.

The results of BAM-AMHG-only applied to the width-discharge data set suggest a mixed picture for Bayesian AMHG vis a vis the previous GA-based AMHG methods. On one hand, this algorithm improved greatly on the maximum RRMSE and did not produce the extreme outliers seen in the GA results. On the other hand, Bayesian AMHG produced higher minimum and median RRMSE. These versions of AMHG differed in their treatment of the parameter Q_c, with the genetic algorithm using a now-defunct "proxy" based on statistics of river width, while BAM assigned this parameter a prior distribution centered (in log space) on water-balance model estimated average discharge. This difference does not account for the genetic algorithm's better performance, as using proxy Q_c with BAM resulted in far less accurate estimates of discharge. In addition, the GA resulted in flatter hydrographs with more consistent flow estimates between cross sections when higher b values were inverted, essentially dampening the hydrograph about Q_c. If this Q_c passed through known flows, then the GA essentially produces a result similar to mean annual flow with dampened dynamic hydrograph response, which results in low error metrics. This result highlights the need to better understand the physical determinants of AMHG, particularly the Q_c parameter.

While this study used Manning's equation and AMHG as flow laws, the BAM framework extends readily to other flow laws, and can be treated as a general framework for conducting inference in underconstrained hydraulic systems using externally derived prior distributions. While multiple flow laws could conceivably be used synergistically—as Manning's and AMHG were in this study—the benefit from such a coupling is likely to be greatest when the physical bases for the flow laws do not overlap.

4.3. AMHG

This study provides the first evidence of the existence and utility of a reach-averaged AMHG. AHG has previously been invoked at the reach scale (e.g., Jowett, 1998), but AMHG has yet to be shown to exist at this scale. This study assumes and indeed shows that AMHG exists at the reach scale, which has heretofore not been shown. We might expect the successful adaptation of AMHG to reaches given the AHG precedent, but these results raise more questions than they answer about the origins of AMHG and its application. For instance, in cases where reaches are short and homogeneous the assumption of AMHG is straightforward at the reach scale. However, the results raise the need for further empirical work investigating AMHG strength when characterized using reach-averaged width and discharge data.

AMHG R^2 (Gleason et al., 2014) for reach data shows that indeed AMHG exists at this scale for a majority of the Durand et al. (2016) test cases, with 15 of 19 rivers having reach-scale AMHG R^2 greater than 0.75. Rivers with strong reach-scale AMHG nearly always had strong cross-section-scale AMHG, and vice versa, and both had similarly strong AMHG on average.

While BAM variants that included Manning's equation outperformed the AMHG-only variant in most rivers, this is not an even-handed comparison, given the availability of data required by each. While both can in theory be used with remotely sensed data, only AMHG is capable of predicting discharge based on currently available satellite data products. Moreover, AMHG produced RRMSE values at or below 35% on five rivers (the best Manning-inclusive variant did so on seven rivers) and indeed had the lowest minimum RRMSE value (9%) of any BAM variant. Given AMHG's status as the only available McFLI method capable of predicting discharge using only width data and this satisfactory performance in certain cases, future work is needed to better discriminate a priori which rivers are likely to have a strong AMHG.

5. Conclusion

The potential of satellite remote sensing to quantify discharge on the world's rivers hinges on the development of algorithms that can determine flow-law parameters using remotely sensed stream width, height, and slope. Progress using the McFLI paradigm for flow-law inversion is hampered by parameter equifinality, requiring either new hydraulic invocations or else a means of selecting from an infinite space of equifinal parameters. This study took the latter approach, describing a set of Bayesian algorithms that constrain the uncertainty of discharge and flow-law parameters using SWOT observations and a priori information. These

algorithms were applied to the estimation of discharge using synthetic, model-derived data in a set of 19 rivers, demonstrating improved accuracy over previous methods. The algorithms were found to have low bias in aggregate, and to have a low range of RRMSE values compared to most other McFLI approaches. More fundamentally, this study demonstrates the applicability of Bayesian inference methods to discharge estimation using remotely sensed river width, slope, and height. The approach formalizes and constrains the uncertainty in both discharge estimates and equation parameters, and is flexible with regard to the flow law(s) employed. Since the posterior uncertainty in discharge and other parameters is constrained using prior information, future efforts to more tightly constrain these priors will further improve on BAM performance. The AMHG-only BAM variant had less consistently strong performance, but performed well in certain cases, highlighting the need to more fully understand AMHG parameters from a physical standpoint, and to be able to discern which rivers possess a strong AMHG without in situ data.

Acknowledgments
This work was funded by NASA SWOT Science Team grant NNX16AH82G to M. T. Durand and C. J. Gleason. All data used herein are available as supporting information to this manuscript, and source code for the BAM method is freely available on GitHub: https://github.com/markwh/bamr.

References

Andreadis, K. M., Clark, E. A., Lettenmaier, D. P., & Alsdorf, D. E. (2007). Prospects for river discharge and depth estimation through assimilation of swath-altimetry into a raster-based hydrodynamics model. *Geophysical Research Letters*, *34*, L10403. https://doi.org/10.1029/2007GL029721

Betancourt, M., & Girolami, M. (2015). Hamiltonian Monte Carlo for hierarchical models. In *Current trends in Bayesian methodology with applications* (Vol. 79, p. 30). Boca Raton, FL: CRC Press.

Biancamaria, S., Durand, M., Andreadis, K. M., Bates, P. D., Boone, A., Mognard, N. M., . . . Clark, E. A. (2011). Assimilation of virtual wide swath altimetry to improve Arctic river modeling. *Remote Sensing of the Environment*, *115*(2), 373–381.

Birkinshaw, S. J., Moore, P., Kilsby, C. G., O'donnell, G., Hardy, A. J., & Berry, P. A. M. (2014). Daily discharge estimation at ungauged river sites using remote sensing. *Hydrological Processes*, *28*(3), 1043–1054. https://doi.org/10.1002/hyp.9647

Bjerklie, D. M., Moller, D., Smith, L. C., & Dingman, S. L. (2005). Estimating discharge in rivers using remotely sensed hydraulic information. *Journal of Hydrology*, *309*(1), 191–209.

Brackenridge, G. R., Ngiem, S. V., Anderson, E., & Chien, S. (2005). Space-based measurement of river runoff. *Eos, Transactions of the American Geophysical Union*, *86*(19), 185–188. https://doi.org/10.1029/2005EO190001

Canova, M. G., Fulton, J. W., & Bjerklie, D. M. (2016). *USGS HYDRoacoustic dataset in support of the surface water oceanographic topography satellite mission (HYDRoSWOT)*. Reston, VA: U.S. Geological Survey. https://doi.org/10.5066/F7D798H6

Durand, M., Andreadis, K., Konstantinos, M., Alsdorf, D., Lettenmaier, D. P., Moller, D., & Wilson, M. (2008). Estimation of bathymetric depth and slope from data assimilation of swath altimetry into a hydrodynamic model. *Geophysical Research Letters*, *35*, L20401. https://doi.org/10.1029/2008GL034150

Durand, M., Gleason, C. J., Garambois, P. A., Bjerklie, D., Smith, L. C., Roux, H., . . . Vilmin, L. (2016). An intercomparison of remote sensing river discharge estimation algorithms from measurements of river height, width, and slope. *Water Resources Research*, *52*, 4527–4549. https://doi.org/10.1002/2015WR018434

Durand, M., Neal, J., Rodríguez, E., Andreadis, K. M., Smith, L. C., & Yoon, Y. (2014). Estimating reach-averaged discharge for the river severn from measurements of river water surface elevation and slope. *Journal of Hydrology*, *511*, 92–104.

Durand, M., Rodriguez, E., Alsdorf, D. E., & Trigg, M. (2010). Estimating river depth from remote sensing swath interferometry measurements of river height, slope, and width. *IEEE Journal of Selected Topics in Applied Earth Observations and Remote Sensing*, *3*(1), 20–31.

Garambois, P.-A., & Monnier, J. (2015). Inference of effective river properties from remotely sensed observations of water surface. *Advances in Water Resources*, *79*, 103–120.

Gelman, A., Carlin, J. B., Stern, H. S., & Rubin, D. B. (2014). *Bayesian data analysis*. Boca Raton, FL: Chapman and Hall.

Gleason, C. J., Garambois, P. A., & Durand, M. T. (2017). Water, satellites, and mass conservation: Tracking river flows from space. *Eos, Transactions American Geophysical Union*, *98*. https://doi.org/10.1029/2017EO078085

Gleason, C. J., & Hamdan, A. N. (2015). Crossing the (watershed) divide: Satellite data and the changing politics of international river basins. *The Geographical Journal*, *183*(1), 2–15. https://doi.org/10.1111/geoj.12155

Gleason, C. J., & Smith, L. C. (2014). Toward global mapping of river discharge using satellite images and at-many-stations hydraulic geometry. *Proceedings of the National Academy of Sciences of the United States of America*, *111*(13), 4788–4791.

Gleason, C. J., Smith, L. C., & Lee, J. (2014). Retrieval of river discharge solely from satellite imagery and at-many-stations hydraulic geometry: Sensitivity to river form and optimization parameters. *Water Resources Research*, *50*, 9604–9619. https://doi.org/10.1002/2014WR016109

Gleason, C. J., & Wang, J. (2015). Theoretical basis for at-many-stations hydraulic geometry. *Geophysical Research Letters*, *42*, 7107–7114. https://doi.org/10.1002/2015GL064935

Hannah, D. M., Demuth, S., van Lanen, H. A. J., Looser, U., Prudhomme, C., Rees, G., . . . Tallaksen, L. M. (2011). Large-scale river flow archives: Importance, current status and future needs. *Hydrological Processes*, *25*(7), 1191–1200. https://doi.org/10.1002/hyp.7794

Jowett, I. G. (1998). Hydraulic geometry of New Zealand rivers and its use as a preliminary method of habitat assessment. *River Research and Applications*, *14*(5), 451–466.

Kennedy, E. (1984). Discharge ratings at gaging stations. In *U.S. Geological Survey, techniques of water-resources investigations*. Reston, VA: U.S. Geological Survey.

LeFavour, G., & Alsdorf, D. (2005). Water slope and discharge in the Amazon River estimated using the shuttle radar topography mission digital elevation model. *Geophysical Research Letters*, *32*, L17404. https://doi.org/10.1029/2005GL023836

Neal, J., Schumann, G., Bates, P., Buytaert, W., Matgen, P., & Pappenberger, F. (2009). A data assimilation approach to discharge estimation from space. *Hydrological Processes*, *23*(25), 3641–3649.

Shen, C., Wang, S., & Liu, X. (2016). Geomorphological significance of at-many-stations hydraulic geometry. *Geophysical Research Letters*, *43*, 3762–3770. https://doi.org/10.1002/2016GL068364

Sivapalan, M., Takeuchi, K., Franks, S. W., Gupta, V. K., Karambiri, H., Lakshmi, V., . . . Zehe, E. (2003). IAHS decade on predictions in ungauged basins (PUB), 2003–2012: Shaping an exciting future for the hydrological sciences. *Hydrological Sciences Journal*, *48*(6), 857–880.

Smith, L. C., Isacks, B. L., Bloom, A. L., & Muray, A. B. (1996). Estimation of discharge from three braided rivers using synthetic aperture radar satellite imagery: Potential application to ungaged basins. *Water Resources Research*, *32*(7), 2021–2034.

Talagrand, O. (2003). Bayesian estimation, optimal interpolation, statistical linear estimation. In R. Swinbank, V. Shutyaev, & W. A. Lahoz (Eds.), *Data assimilation for the earth system, NATO science series IV* (Vol. 26, pp. 21–35). Dordrecht, the Netherlands: Kluwer Academic.

Tourian, M. J., Sneeuw, N., & Bárdossy, A. (2013). A quantile function approach to discharge estimation from satellite altimetry (ENVISAT). *Water Resources Research*, *49*, 4174–4186. https://doi.org/10.1002/wrcr.20348

Wisser, D., Fekete, B., Vörösmarty, C., & Schumann, A. (2010). Reconstructing 20th century global hydrography: A contribution to the global terrestrial network-hydrology (GTN-H). *Hydrology and Earth System Sciences*, *14*(1), 1–24.

Yoon, Y., Durand, M., Merry, C. J., Clark, E. A., Andreadis, K. M., & Alsdorf, D. E. (2012). Estimating river bathymetry from data assimilation of synthetic SWOT measurements. *Journal of Hydrology*, *464*, 363–375.